tion domain binding protein and was shown to coactivate JUN-mediated gene expression (*24*). Recently, mammalian JAB1 was reported to bind a number of other proteins: The lutropin/choriogonadotropin receptor (*25*) and CDK inhibitor p27 (*26*) are targeted for degradation by JAB1, whereas signals propagated by the LFA1 integrin (*27*) and MIF cytokine (*28*) modulate JAB1 by an unknown mechanism(s). Our work suggests that a key function of the JAB1-containing CSN is to promote cleavage of NEDD8 from cullins and other NEDD8-modified proteins, and that the defects of CSN mutants arise from a failure to cleave NEDD8 from specific substrates. For example, failure to remove NEDD8 from COP1, HY5, or an affiliated protein may constitutively activate light-dependent gene expression in *A. thaliana* by blocking COP1-dependent turnover of the photomorphogenetic regulator HY5 (*29*).

The functional impact of CSN on its substrates is difficult to predict. NEDD8 attachment is essential in vivo (*19*) and promotes $SCF^{\beta\text{-TRCP}}$ activity in vitro (*3*), but conversely, diminished CSN function inhibits turnover of an SCF^{TIR1} target in *A. thaliana* (*30*). Thus, NEDD8 may need to be cyclically attached to and cleaved from CUL1 for optimal SCF function. Cycles of neddylation, like cycles of protein phosphorylation, may serve different functions in different contexts. Nonetheless, given the potentially large number of cullin-based ubiquitin ligases and the observed accumulation of additional NEDD8-modified proteins in Δ*caa1* cells, CSN is likely to modulate a broad range of biological processes.

References and Notes

1. R. J. Deshaies, *Annu. Rev. Cell Dev. Biol.* **15**, 435 (1999).
2. V. Podust *et al.*, *Proc. Natl. Acad. Sci. U.S.A.* **97**, 4579 (2000).
3. M. Read *et al.*, *Mol. Cell. Biol.* **20**, 2326 (2000).
4. K. Wu, A. Chen, Z. Pan, *J. Biol. Chem.* **275**, 32317 (2000).
5. M. Morimoto, T. Nishida, R. Honda, H. Yasuda, *Biochem. Biophys. Res. Commun.* **270**, 1093 (2000).
6. Supplementary information is available at *Science* Online (www.sciencemag.org/cgi/content/full/1059780/DC1).
7. A. Shevchenko, M. Wilm, O. Vorm, M. Mann, *Anal. Chem.* **68**, 850 (1996).
8. J. H. Seol, A. Shevchenko, A. Shevchenko, R. J. Deshaies, *Nature Cell Biol.* **3**, 384 (2001).
9. A. Shevchenko, A. Loboda, W. Ens, K. G. Standing, *Anal. Chem.* **72**, 2132 (2000).
10. X. Deng *et al.*, *Trends Genet.* **16**, 202 (2000).
11. N. Wei, X. Deng, *Trends Genet.* **15**, 98 (1999).
12. N. Wei *et al.*, *Curr. Biol.* **8**, 919 (1998).
13. M. Seeger *et al.*, *FASEB J.* **12**, 469 (1998).
14. M. Glickman *et al.*, *Cell* **94**, 615 (1998).
15. S. E. Schwarz, unpublished data.
16. Animal and *A. thaliana* proteins are referred to as ABC (e.g., CUL1, NEDD8) and yeast and *B. napus* proteins are referred to as Abc (e.g., Pcu1, Nedd8) to conform to existing nomenclature and make it easier to discern the origin of proteins referred to in the text.
17. K. Mundt *et al.*, *Curr. Biol.* **9**, 1427 (1999).
18. C. Zhou, D. A. Wolf, unpublished data.
19. F. Osaka *et al.*, *EMBO J.* **19**, 3475 (2000).
20. The reduced level of neddylation observed for wild-type Pcu1 in Fig. 2B, as compared to Fig. 2A, most likely results from saturation of the neddylation pathway by overproduction of Pcu1 from the *nmt1*$^+$ promoter.
21. R. Verma, unpublished data.
22. We propose, on the basis of mononeddylation of cullins, that each band represents a discrete polypeptide (as opposed to multineddylated forms of a single protein).
23. G. A. Cope, R. J. Deshaies, unpublished data.
24. F. Claret, M. Hibi, S. Dhut, T. Toda, M. Karin, *Nature* **383**, 453 (1996).
25. S. Li, X. Liu, M. Ascoli, *J. Biol. Chem.* **275**, 13386 (2000).
26. K. Tomoda, Y. Kubota, J. Kato, *Nature* **398**, 160 (1999).
27. E. Bianchi *et al.*, *Nature* **404**, 617 (2000).
28. R. Kleemann *et al.*, *Nature* **408**, 211 (2000).
29. M. Osterlund, C. Hardtke, N. Wei, X. Deng, *Nature* **405**, 462 (2000).
30. C. Schwechheimer *et al.*, *Science* **291**, 1379 (2001).
31. Manipulations of *S. pombe* and indirect immunofluorescence were performed according to protocols published at www.bio.uva.nl/pombe/handbook.
32. S. Lyapina, C. Correll, E. Kipreos, R. Deshaies, *Proc. Natl. Acad. Sci. U.S.A.* **95**, 7451 (1998).
33. N. Wei, X. Deng, *Photochem. Photobiol.* **68**, 237 (1998).

34. We thank C. Lois, J Roberts, T. Caspari, A. Carr, S. Forsburg, J. Thorner, T. Toda, F. Osaka, Y. Xiong, and P. Nurse for generously providing retroviral vectors, *S. pombe* strains, expression plasmids, and antibodies; M. Petroski for ^{32}P-labeled ubiquitin; and R. Verma for experimental input, helpful discussions, and pointing out JAB1 homology to ubiquitin-specific proteases. We also thank P. Jackson and members of his laboratory for hosting this project in its early days. Supported by an Amgen fellowship (S.L.) and by the W. M. Keck Foundation and HHMI.

12 February 2001; accepted 17 April 2001
Published online 3 May 2001;
10.1126/science.1059780
Include this information when citing this paper.

Genetic Analysis of Digestive Physiology Using Fluorescent Phospholipid Reporters

Steven A. Farber,[1,2]*†‡ Michael Pack,[3]*† Shiu-Ying Ho,[2] Iain D. Johnson,[5] Daniel S. Wagner,[4] Roland Dosch,[4] Mary C. Mullins,[4] H. Stewart Hendrickson,[6] Elizabeth K. Hendrickson,[6] Marnie E. Halpern[1]

Zebrafish are a valuable model for mammalian lipid metabolism; larvae process lipids similarly through the intestine and hepatobiliary system and respond to drugs that block cholesterol synthesis in humans. After ingestion of fluorescently quenched phospholipids, endogenous lipase activity and rapid transport of cleavage products results in intense gall bladder fluorescence. Genetic screening identifies zebrafish mutants, such as *fat free*, that show normal digestive organ morphology but severely reduced phospholipid and cholesterol processing. Thus, fluorescent lipids provide a sensitive readout of lipid metabolism and are a powerful tool for identifying genes that mediate vertebrate digestive physiology.

To assay lipid metabolism in living larvae, we synthesized fluorescently tagged or quenched phospholipids (Figs. 1A and 2A). Such modified lipids are effective substrates for phospholipase A_2 (PLA_2) cleavage and sensitive reporters of enzymatic activity in vivo (*1, 2*). PLA_2 was targeted because of its importance in the generation of lipid signaling molecules, host defenses, lipid absorption, and cancer (*3–5*). Given the shared features of lipid processing in mammals and teleosts (*6, 7*), zebrafish mutagenesis screens using lipid reporters should identify genes relevant to human lipid metabolism and disease.

Reporters were constructed by covalently linking fluorescent moieties to sites adjoining the cleavage site of phospholipids. Dye-dye or dye-quencher interactions modify fluorescence without impeding enzyme-substrate interactions (*8*). PLA_2 cleavage results in immediate unquenching and detectable fluorescence. Quenched phospholipids [*N*-((6-(2,4-dinitro-

[1]Department of Embryology, Carnegie Institution of Washington, Baltimore, MD 21210, USA. [2]Department of Microbiology and Immunology, Kimmel Cancer Center, Thomas Jefferson University, Philadelphia, PA 19107, USA. [3]Department of Medicine, [4]Department of Cell and Developmental Biology, University of Pennsylvania, Philadelphia, PA 19104, USA. [5]Molecular Probes Inc., Eugene, OR 97402, USA. [6]Department of Chemistry, University of Washington, Seattle, WA 98133, USA.

*These authors contributed equally to this work.
†To whom correspondence should be addressed. E-mail: sfarber@lac.jci.tju.edu, mpack@mail.med.upenn.edu
‡Present address: Department of Microbiology and Immunology, Kimmel Cancer Center, Thomas Jefferson University, Philadelphia, PA 19107, USA.

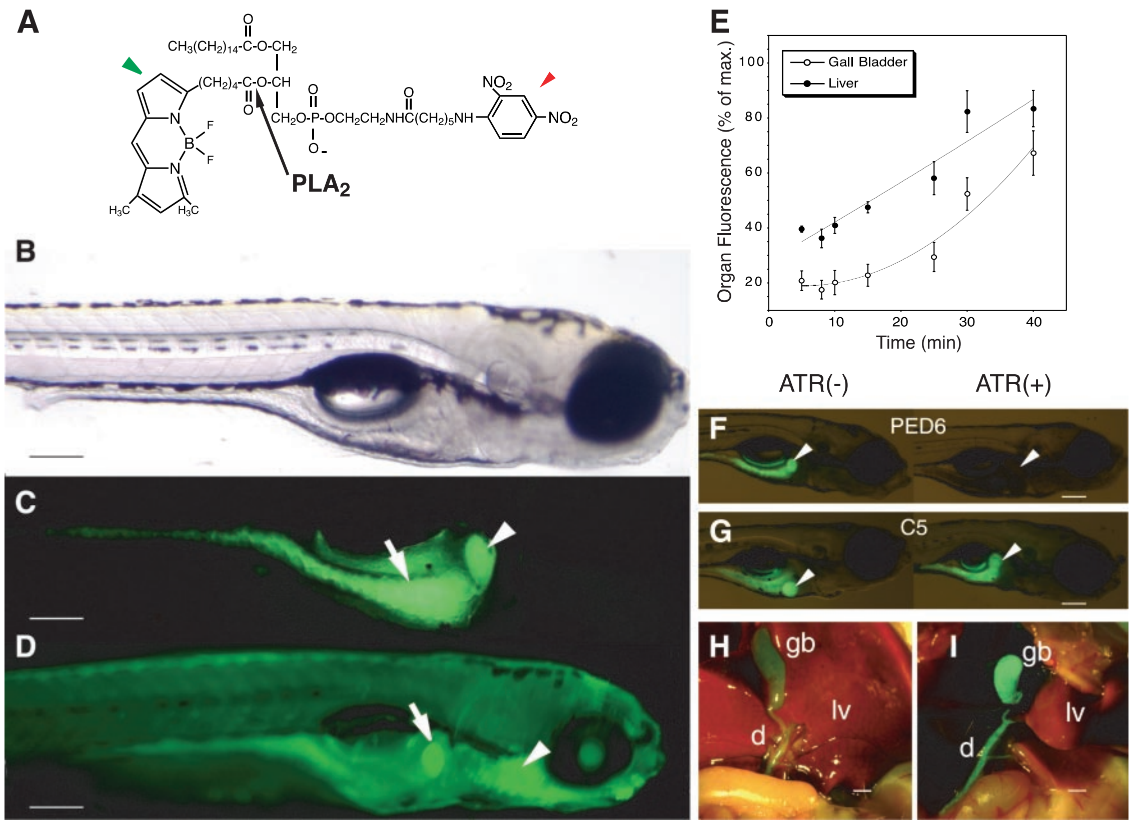

Fig. 1. PED6, a fluorescent PLA$_2$ reporter. (**A**) Dinitrophenyl on the phospholipid head group (red arrowhead) quenches emission of the BODIPY-labeled acyl chain (excitation 505 nm) (green arrowhead). PLA$_2$ cleavage (arrow) liberates the BODIPY-acyl chain, resulting in unquenching and green fluorescent emission. (**B**) Bright-field image of a 5 dpf larva soaked in PED6 (0.3 μg/ml, 2 hours). (**C**) Corresponding fluorescent image, with intestinal (arrow) and gall bladder (arrowhead) labeling. (**D**) Larva soaked in BODIPY-C5-PC (0.2 μg/ml). In contrast to (C), unquenched fluorescent lipid labels the pharynx (arrowhead), confirming that lipid is swallowed before gall bladder labeling (arrow). (**E**) Organ fluorescence intensity determined at specific times was normalized to intensity at 45 min. Data are expressed as means ± SEM. (**F** and **G**) Atorvastatin (ATR) inhibits processing of PED6 (F) but not of BODIPY FL-C5 (Molecular Probes) (G). Larvae were bathed in fluorophore (0.6 μM) in the presence or absence of atorvastatin (Lipitor tablet suspension containing 1 mg/ml) (arrowhead, gall bladder). (**H**) Mouse digestive organs. (**I**) Gall bladder fluorescence after processing (t = 30 min) of PED6 (1 μg), administered by gavage. Symbols: gb, gall bladder; d, common bile duct; lv, liver. Scale bars, 1.0 mm (H and I), 200 μm (other images).

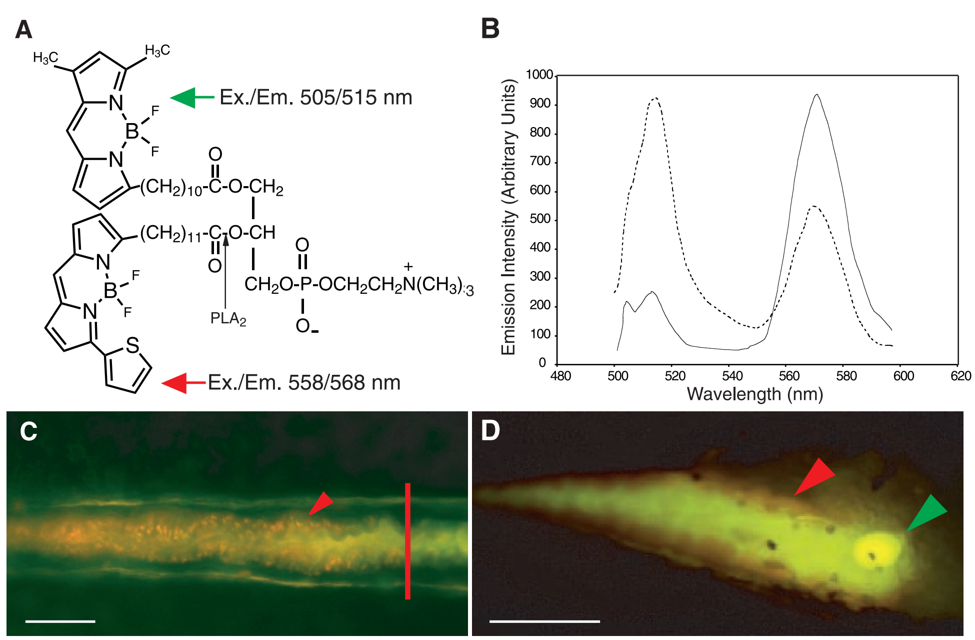

Fig. 2. BODIPY FR-PC reporter reveals both substrate and cleavage products. (**A**) Upon integration into cells, excitation (505 nm) results in orange (568-nm) emission due to FRET. After PLA$_2$ cleavage (arrow), 515-nm emission (green) is observed. (**B**) Fluorescence emission spectrum of BODIPY FR-PC (excitation, 505 nm) with peaks at 515 and 568 nm indicative of FRET. Solid line, before addition of PLA$_2$; dashed line, after addition of *Naja. naja* PLA$_2$. (**C**) Fluorescence of a 5 dpf larva after BODIPY FR-PC (5 μg/ml) labeling: Visualization of segment II enterocytes (left of red bar) after pinocytosis of uncleaved BODIPY FR-PC (1 hour after labeling). Arrowhead indicates the segment II domain. Green gall bladder fluorescence is not shown. (**D**) After 4 hours, BODIPY FR-PC metabolites reside in the gall bladder (green emission, green arrowhead). Uncleaved substrate (orange emission, red arrowhead) is observed in the anterior intestinal epithelium. Scale bars, 200 μm.

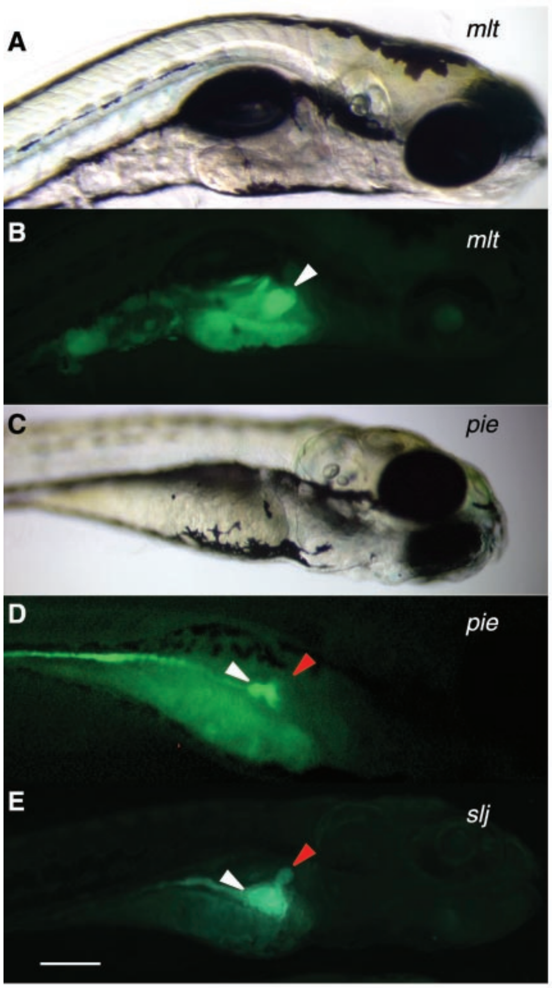

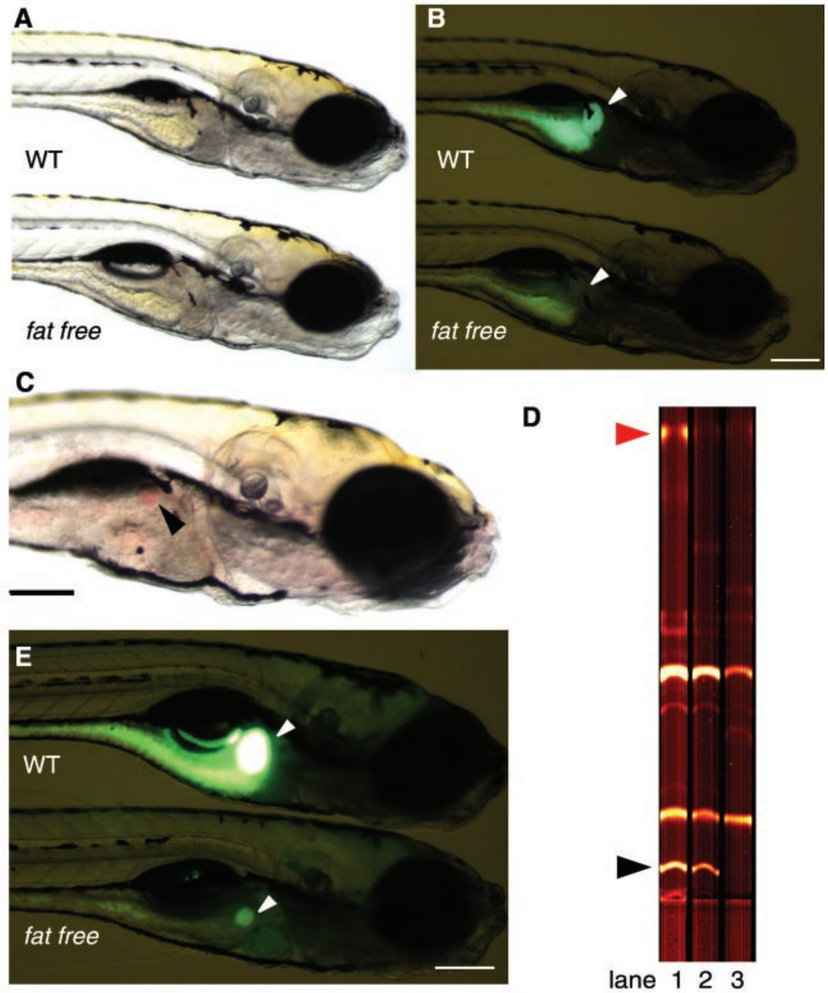

Fig. 3 (left). Lipid processing in intestinal mutants. (**A** and **C**) Bright-field images of *mlt* and *pie* larvae (5 dpf). (**B** and **D**) Fluorescent images corresponding to (A) and (C). Normal lipid processing of PED6 (0.3 μg/ml, 2 hours) occurs in *mlt* larva (arrowhead marks gall bladder). Abnormal lipid processing is seen in PED6-labeled *pie* (D) and *slj* (**E**) larvae; fluorescence is present in the intestinal lumen (white arrowhead) and reduced in the gall bladder (red arrowhead). Scale bar, 200 μm. **Fig. 4 (right).** *fat free* larvae lack gall bladder fluorescence. (**A**) Bright-field images of wild-type (WT) and mutant 5 dpf larvae. (**B**) Corresponding fluorescent image of the gall bladder after PED6 labeling (0.3 μg/ml) (arrowheads). (**C**) Biliary secretion of phenol red in *fat free* larvae. Mutant larvae identified by PED6 labeling were injected with phenol red as described (*26*) (arrowhead, gall bladder). (**D**) Reduced lipid processing in *fat free* mutants. TLC of the pooled lipid fraction from eight larvae is shown after labeling with BODIPY C5-PC (12 hours, 0.16 μg/ml); red arrowhead denotes BODIPY-cholesteryl ester, black arrowhead indicates BODIPY C5-PC (lane 1, WT; lane 2, *fat free*; lane 3, endogenous fluorescent lipids present in unlabeled WT larvae). TLC: solvent system 1 (chloroform: methanol:water; 35:7:0.7); solvent system 2 (ethyl ether:benzene: ethanol:acetic acid; 40:50:2:0.2). (**E**) *fat free* larvae fail to accumulate 22-[*N*-(7-nitrobenz-2-oxa-1,3-diazol-4-yl)amino]-23,24-bisnor-5-cholen-3-ol (NBD-cholesterol) (2 hours, 3 μg/ml, solubilized with fish bile). Scale bars, 200 μm.

phenyl)amino)hexanoyl)-1-palmitoyl-2-BODIPY-FL-pentanoyl-*sn*-glycero-3-phosphoethanolamine (PED6) (*2*)] allow subcellular visualization of PLA_2 activity in zebrafish embryos (*1*) and reveal organ-specific activity (*9*). Larvae [5 days post-fertilization (dpf)] bathed in PED6 show intense gall bladder fluorescence and, shortly thereafter, intestinal luminal fluorescence (Fig. 1C).

Larvae were bathed in an unquenched fluorescent lipid to confirm that lipids were swallowed (Fig. 1D). We determined that PED6 is cleaved within the intestine, because PLA_2 activity was not detected in bile (*10*) and fluorescent PED6 metabolites underwent rapid hepatobiliary transport, labeling the liver before the gall bladder (Fig. 1E). Moreover, PED6 labeling of the gall bladder was completely blocked by atorvastatin (Lipitor, Parke-Davis) (Fig. 1F), a potent inhibitor of cholesterol synthesis in humans (*11*). Because the addition of exogenous bile reversed this effect (*12*), and atorvastatin failed to inhibit processing of a water-soluble short-chain fatty acid (BODIPY FL-C5, Molecular Probes Inc.) (*7*) (Fig. 1G), we hypothesize that atorvastatin blocks the synthesis of cholesterol-derived biliary emulsifiers needed for dietary lipid absorption (*13, 14*). These results, coupled with the rapid appearance of biliary fluorescence in mice fed PED6 (Fig. 1, H and I), demonstrate that PED6 metabolism in zebrafish corresponds to established mechanisms of lipid processing in mammals (*15*).

To determine the site of PLA_2 activity more precisely, we developed a substrate [BODIPY FR-PC (Fig. 2A)] that emits distinct fluorescent profiles before and after cleavage (*16*). This phospholipid contains two dyes that interact via fluorescence resonance energy transfer (FRET) (*17*). The substrate and cleavage product have unique spectral signatures, allowing their tissue distribution to be distinguished by fluorescence microscopy. Excitation (505 nm) of micelle-incorporated BODIPY FR-PC produces an orange emission (568 nm; Fig. 2B) from the *sn2* fluorophore via the FRET effect (*18*). However, cleavage of the substrate by purified PLA_2 releases the *sn2* acyl chain and abolishes FRET (Fig. 2B). Excitation of the resultant lysolipid produces a green emission (515 nm).

Within 1 hour, larvae bathed in BODIPY FR-PC showed a bright green fluorescent gall bladder and orange fluorescence within the apical cytoplasm of posterior intestinal cells (Fig. 2C). These cells are known to absorb luminal macromolecules through pinocytosis (*19*). Orange fluorescence indicative of uncleaved substrate was also observed in the anterior intestine epithelium, the site of lipid absorption in fish (*6, 20*). FRET emission (orange) was never detected in the liver even after prolonged incubation (Fig. 2D), supporting the hypothesis that gall bladder fluorescence after ingestion of labeled lipids is due to cleavage by intestinal PLA_2.

To use fluorescent lipid assays for genetic screening, we first examined PED6 processing in mutants known to perturb intestinal morphology in a region-specific manner (*21*). The mutations *slim jim* (*slj*) and *piebald* (*pie*) each cause degeneration of anterior intestinal epithelium and exocrine pancreas, whereas *meltdown* (*mlt*) results in cystic expansion of the posterior intestine. As shown in Fig. 3, A and B, *mlt* mutants retain PED6 processing in the anterior intestine and show normal levels of gall bladder fluorescence. In contrast, *pie* (Fig. 3, C and D) and *slj* (Fig. 3E) mutants display greatly reduced gall bladder labeling. Hence, fluorescent lipids can be used to identify mutants with abnormal digestive organ morphology.

Lipid reporters have also proven effective for identifying mutations that perturb lipid metabolism without causing obvious morphological defects. In a pilot screen, larval progeny of individual F_2 families derived from an ENU mutagenesis protocol (*22*) were bathed in PED6 and screened for digestive organ morphology and phospholipid processing. PED6 fluorescent metabolites enhance visibility of digestive organ structure, facilitating scoring of gall bladder development, intestinal folding, and bile duct morphology (*23*). Of the 190 genomes screened, two mutations were identified and confirmed in the subsequent generation. The recessive lethal mutation *canola* produces a phenotype closely resembling that of *slj* and *pie*, with degeneration of the intestinal epithelium and reduced gall bladder and intestinal fluorescence (*24*). The *fat free* recessive lethal mutation causes a more pronounced reduction in fluorescence (Fig. 4B) . However, in contrast to *canola* and other intestinal mutants, the *fat free* digestive tract has a normal appearance at 5 dpf (Fig. 4A). Therefore, *fat free* would have escaped detection in a screen based solely on morphological criteria.

To determine how the *fat free* mutation affects larval digestive physiology, we first determined that swallowing was normal in mutants by their ingestion of fluorescent beads (*25*). Next, we demonstrated that the *fat free* hepatobiliary system was functional by monitoring biliary excretion of the organic anion phenol red (Fig. 4C) (*26*). Thin-layer chromatography (TLC) of metabolites produced by *fat free* larvae labeled with an unquenched BODIPY phosphatidylcholine analog (*1*) revealed that PLA_2 processing was intact (*27*). However, extracts prepared from mutants contained significantly reduced levels of fluorescent cleavage products (Fig. 4D).

Lipid processing was further examined using a fluorescent cholesterol analog (*28*) whose absorption is dependent on biliary emulsification. Cholesterol was poorly absorbed by *fat free* larvae (Fig. 4E). Because uptake of BODIPY FL-C5, a more soluble short-chain fatty acid, was reduced to a lesser extent than uptake of cholesterol and PED6 (*24*), we propose that *fat free* directly regulates bile synthesis or secretion rather than intestinal lipid absorption or transport. Further, the zebrafish *fat free* mutation provides in vivo evidence supporting the hypothesis, derived from mammalian cell culture experiments, that phospholipid turnover and cholesterol metabolism are coupled (*29*).

Mutagenesis screens using fluorescent lipids exploit the advantages of zebrafish for combining genetic analyses with imaging of enzymatic function. The existence of related lipid processing mechanisms in mammals and teleosts, and the finding that therapeutic drugs used to modify lipid metabolism in humans are active in zebrafish, suggest that genetic screens can be designed to probe the mechanistic basis of acquired and heritable human disorders. Fluorescent reporters are predicted to identify genes involved in diseases of lipid metabolism, such as atherosclerosis; in disorders of biliary secretion, such as biliary atresia; and in cancer, a disease in which lipid signaling plays an important role.

References and Notes

1. S. A. Farber, E. S. Olson, J. D. Clark, M. E. Halpern, *J. Biol. Chem.* **274**, 19338 (1999).
2. H. S. Hendrickson, E. K. Hendrickson, I. D. Johnson, S. A. Farber, *Anal. Biochem.* **276**, 27 (1999).
3. M. MacPhee *et al.*, *Cell* **81**, 957 (1995).
4. R. T. Cormier *et al.*, *Nature Genet.* **17**, 88 (1997).
5. E. A. Dennis, *Trends Biochem. Sci.* **22**, 1 (1997).
6. D. Tocher, in *Biochemistry and Molecular Biology of Fishes*, P. Hochachka, T. Mommsen, Eds. (Elsevier, New York, 1995), vol. 4, pp. 119–157.
7. M. A. Sheridan, *Comp. Biochem. Physiol. B* **90**, 679 (1988).
8. H. S. Hendrickson, *Anal. Biochem.* **219**, 1 (1994).
9. Larvae were labeled in embryo medium (EM) [M. Westerfield, *The Zebrafish Book* (Univ. of Oregon, Eugene, OR, ed. 3, 1995)], anesthetized (tricaine, 170 μg/ml), and placed in depression slides. Fluorescent images were captured over 1 hour using a Zeiss Axiocam 2 mounted on a Leica MZFL-III.
10. Dissected adult gall bladders were lysed in EM (30 μl) containing BODIPY FL-C5-PC (0.1 μg) to release bile. PLA_2 activity was determined as described (*1*). Measurements were compared with activity of bile-depleted gall bladders.
11. J. W. Nawrocki *et al.*, *Arterioscler. Thromb. Vasc. Biol.* **15**, 678 (1995).
12. Bile obtained from freshly killed tilapia (*Orechromis mossambicus*) was extracted with three volumes of methanol:chloroform (1:2). The aqueous fraction was recovered, reduced to one volume under nitrogen, and added to EM (20 μl/ml).
13. Dissected adult gall bladders ($n = 5$) were dissolved in isopropanol and subjected to mass spectrometry. The dominant biliary emulsifier was identified as 5α-cyprinol sulfate, a cholesterol-derived C_{27} bile alcohol (A. F. Hofmann and L. R. Hagey, personal communication).
14. T. Goto *et al.*, *Hepatology* **26**, 295A (1997).
15. M. Rubin, R. Pakula, T. Gilat, A. Tietz, *Lipids* **34**, 571 (1999).
16. For methods, see *Science* Online (www.sciencemag.org/cgi/content/full/292/5520/1385/DC1).
17. P. R. Selvin, *Nature Struct. Biol.* **7**, 730 (2000).
18. For determination of the fluorescence emission spectrum of BODIPY FR-PC, mixed micelles of 0.05 mol % BODIPY FR-PC in dimyristoyl phosphatidylcholine (46 mol %) and ditetradecylphosphatidylmethanol (54 mol %) were prepared in buffer [50 mM tris (pH 8), 100 mM NaCl, and 1 mM $CaCl_2$] by sonication of the dried lipids.
19. H. W. Stroband, H. van deer Meer, L. P. Timmermans, *Histochemistry* **64**, 235 (1979).
20. R. E. Honkanen, M. W. Rigler, J. S. Patton, *Am. J. Physiol.* **249**, 399 (1985).
21. M. Pack *et al.*, *Development* **123**, 321 (1996).
22. M. C. Mullins, M. Hammerschmidt, P. Haffter, C. Nusslein-Volhard, *Curr. Biol.* **4**, 189 (1994).
23. To view time-lapse movies of gall bladder contraction and intestinal motility after PED6 labeling, see *Science* Online (www.sciencemag.org/cgi/content/full/292/5520/1385/DC1).
24. S. A. Farber, M. Pack, unpublished data.
25. Larvae (6 dpf) were placed in EM containing fluorescent latex microspheres (0.0025% Fluoresbrite plain YG 2.0 μm, Polysciences Inc.) for 1 hour, washed, and imaged as described (9). Numbers of beads were 10 ± 2 in the wild type versus 14 ± 3 beads in mutant larvae (mean ± SEM, $n = 9$, $P > 0.3$).
26. Phenol red (2% in EM) was injected (~5 nl) into larvae dorsal to the anterior intestine, and labeling of the gall bladder was monitored.
27. For quantification of fluorescence data, see *Science* Online (www.sciencemag.org/cgi/content/full/292/5520/1385/DC1).
28. A. Frolov *et al.*, *J. Biol. Chem.* **275**, 12769 (2000).
29. R. Homan, M. K. Jain, in *Intestinal Lipid Metabolism*, C. M. Mansbach, P. Tso, A. Kuksis, Eds. (Kluwer Academic, New York, 2001), pp. 81–104.

30. Supported by a National Research Service Award (NRSA) and a Barbara McClintock Fellowship (Carnegie Institution) (S.A.F.), National Institute of Diabetes and Digestive and Kidney Diseases grant DK 54942 (M.P.), a NRSA (D.S.W.), the Deutscher Akademischer Austauschdienst (R.D.), the March of Dimes (M.C.M.), NSF grant MCB-9619859 (H.S.H.), and a Pew Scholar's Award (M.E.H.). We thank A. Dolan, M. Macurak, J. Thorpe, R. DeRose, T. Woodard, and D. Hooper for technical assistance and L. R. Hagey and A. F. Hofmann for mass spectrometry analysis of zebrafish bile.

5 March 2001; accepted 11 April 2001

Genetic Analysis of Digestive Physiology Using Fluorescent Phospholipid Reporters

Steven A. Farber, Michael Pack, Shiu-Ying Ho, Iain D. Johnson, Daniel S. Wagner, Roland Dosch, Mary C. Mullins, H. Stewart Hendrickson, Elizabeth K. Hendrickson and Marnie E. Halpern

Science **292** (5520), 1385-1388.
DOI: 10.1126/science.1060418